

Supporting Information

A novel combined chemical kinetic and trapping approach for understanding the correlations between chemical reactivity and interfacial H₂O, Br⁻ and H⁺ ion molarities within CTAB/C₁₂E₆ mixed micelles

Aijaz Ahmad Dar, Laurence S. Romsted, Nighat Nazir, Yongliang Zhang, Xiang Gao, Qing Gu, Changyao Liu

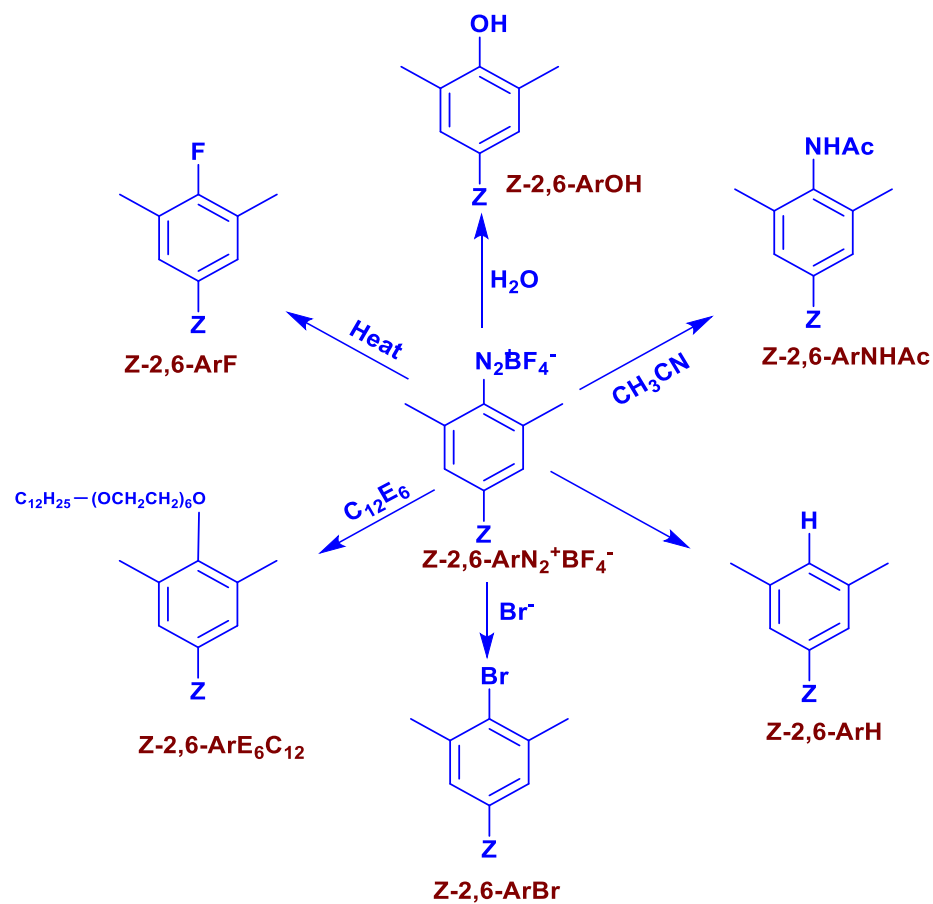
Table of Contents

Page no.

Scheme 1S: Structure and names of the dediazonation products from 16-2,6-ArN ₂ ⁺ formed in CTAB/C ₁₂ E ₆ mixed micelles or from 1-2,6-ArN ₂ ⁺ formed in TMABr/E ₄ aqueous solutions at 27 ± 0.1 °C and [HBr] = 0.032 M (ca. pH = 1.5).	S3
Figure 1S: Chromatograms showing retention times of the various products obtained during dediazonation of 16-2,6-ArN ₂ ⁺ in CTAB/C ₁₂ E ₆ mixed micelles at various mole fractions of C ₁₂ E ₆ (from 0 to 1) at 30 mM total surfactant concentration carried out at 27 ± 0.1 °C and [HBr] = 0.032 M (ca. pH = 1.5). HPLC chromatograms were obtained for product solutions (100 µL) in triplicate at λ = 220 nm using the eluting solvent, 36%/64% (v/v) <i>i</i> -PrOH/MeOH with flow rate of 0.40 mL/min.	S4
Figure 2S: Chromatograms showing retention times of the various products obtained during dediazonation of 1-2,6-ArN ₂ ⁺ in TMABr (A); in E ₄ (B); and TMABr/E ₄ mixture at TMABr mole fraction ≈ 0.2 (C) at total [TMABr] or [E ₄] or [TMABr + E ₄] of 2.5 M at 27 ± 0.1 °C and [HBr] = 0.032 M (ca. pH = 1.5). HPLC chromatograms of the samples (50 µL) were obtained in triplicate at λ = 230 nm using the eluting solvent, 80%/20% (v/v) MeOH/H ₂ O at the flow rate of 0.60 mL/min.	S5
Table 1S: HPLC Average peak areas, observed yields, normalized yields for reaction of 16-ArN ₂ ⁺ in aqueous CTAB/C ₁₂ E ₆ solutions at different mole fractions, X _{C₁₂E₆} , of C ₁₂ E ₆ in solutions at three different total surfactant concentration of 20, 30 and 40 mM at 27°C and [HBr] = 0.032 M. ^a	S6-S7
Table 2S: HPLC Average peak areas, observed yields, normalized yields for reaction of 1-ArN ₂ ⁺ in aqueous TMABr/E ₄ solutions at different mole fractions, X _{E₄} (= 1-X _{TMABr}), of tetraethylene glycol, E ₄ , in solutions at total TMABr and E ₄ concentration of 2.5 M at 27°C and [HBr] = 0.032 M. ^a	S8
Figure 3S: Plot between (a) total bromide ion concentration, [Br _t ⁻] and 1-2,6-ArBr normalized %yield fitted to equation [Br _t ⁻] = -0.220 + 0.220e ^{-(1-2,6-ArBr % yield)/14.45} ; and (b) selectivity of 1-2,6-ArN ₂ ⁺ ion towards bromide ions relative to water, S _W ^{Br} fitted to the equation: S _W ^{Br} = 7.927 + 13.92e ^{-[Br_t⁻]/0.944} as a function of mole fraction of TMABr in TMABr + E ₄ mixture at 27 °C.	S9

- Table 3S:** Estimated values of interfacial molarities of bromide ions and water ($(\text{Br})_m$ and $(\text{H}_2\text{O})_m$) in aqueous CTAB/ C_{12}E_6 solutions at different mole fractions, $X_{\text{C}_{12}\text{E}_6}$, of C_{12}E_6 in solutions at three different total surfactant concentration of 20, 30 and 40 mM at 27°C and $[\text{HBr}] = 0.032 \text{ M}$. **S10**
- Table 4S:** Values of rate constants, A_i 's and the percent contributions of each rate constant to overall rate obtained by fitting kinetic data for reaction of 16 – ArN_2^+ and TBHQ in mixed micelles to equation (3). The total surfactant concentration was fixed at 20 mM, 30 mM and 40 mM and the mole fraction of C_{12}E_6 varied between 0 to 1 in each set of mixed micelles. Reaction conditions were: $[16 - \text{ArN}_2^+] = 5.6 \times 10^{-5} \text{ M}$, $[\text{TBHQ}] = 6.13 \times 10^{-4} \text{ M}$, $[\text{HBr}] = 0.032 \text{ M}$ (pH = 1.5) and $T = 27 \text{ }^\circ\text{C}$. **S11-S12**
- Figure 4S:** Representative plots of absorbance (Z-axis) vs time (x-axis) for reaction of 1- ArN_2^+ with TBHQ at different concentrations of TMABr or E_4 (Y-axis) at pH = 3.45 by using HBr at 27 °C. **S13**
- Figure 5S:** Representative plots of absorbance vs time of 1- ArN_2^+ with TBHQ at (a) different mole fractions of TMABr, X_{TMABr} , in mixture of TMABr + E_4 with pH = 3.45 maintained by using HBr and (b) different pH values using different stoichiometric concentrations of HBr while maintaining mole fraction of TMABr in mixture of TMABr + E_4 equal to 0.5 at 27 °C. Total concentration of TMABr + E_4 in all solutions is 1.25 M. **S14**
- Figure 6S:** Variation of the % observed yields of 16-2,6- ArOH and 16-2,6- ArNHAc obtained during chemical trapping experiments as a function of the mole fraction of C_{12}E_6 in CTAB/ C_{12}E_6 mixed micelles at three different total surfactant concentrations of 20, 30 and 40 mM at 27 °C. **S15**
- Figure 7S:** Variation of k_1' , k_2 and k_3 of reaction between TBHQ^- and 16- ArN_2^+ at micelle-water interface as a function of the mole fraction of C_{12}E_6 in the mixed micelles of CTAB/ C_{12}E_6 at three different total surfactant concentrations of a) 20 mM, b) 30 mM and c) 40 mM at 27 °C. **S16**
- Figure 8S:** Estimated interfacial pH in CTAB- C_{12}E_6 mixed micelles vs the $X_{\text{C}_{12}\text{E}_6}$ a) using the $k_{obs(s)}^{Av}$ vs pH variation in the reaction between 1- ArN_2^+ and TBHQ in the 50/50 TMABr/ E_4 mixture at their total concentration of 1.25 M, and b) from equation 18 obtained from Donnan equilibrium and using the chemical trapping data. The trends in both estimates of $(\text{H})_m$ ($\text{pH} = -\log (\text{H})_m$) are the same although the two differ at low $X_{\text{C}_{12}\text{E}_6}$. **S17**
- Section 1S:** Estimation of the rate constants for the reaction of 16- ArN_2^+ and TBHQ^- in CTAB/ C_{12}E_6 mixed micelles shown in Scheme 2. **S18-S21**
- Section 2S:** Estimation of interfacial hydrogen ion concentration, $(\text{H})_m$ from measured rate constants and the interfacial K_a^m of TBHQ with increasing $X_{\text{C}_{12}\text{E}_6}$ in mixed CTAB/ C_{12}E_6 micelles. **S21**
- Section 3S:** Calculation of bulk aqueous bromide ion concentration, $[\text{Br}]_w$ from the degree of counterion binding with increasing $X_{\text{C}_{12}\text{E}_6}$ in mixed CTAB/ C_{12}E_6 micelles. **S22**

Scheme 1S: Structure and names of the dediazonation products from 16-2,6-ArN₂⁺ formed in CTAB/C₁₂E₆ mixed micelles or from 1-2,6-ArN₂⁺ formed in TMABr/E₄ aqueous solutions at 27 ± 0.1 °C and [HBr] = 0.032 M (ca. pH = 1.5).



Z = C₁₆H₃₃ for long chain probe
 Z = CH₃ for short chain probe

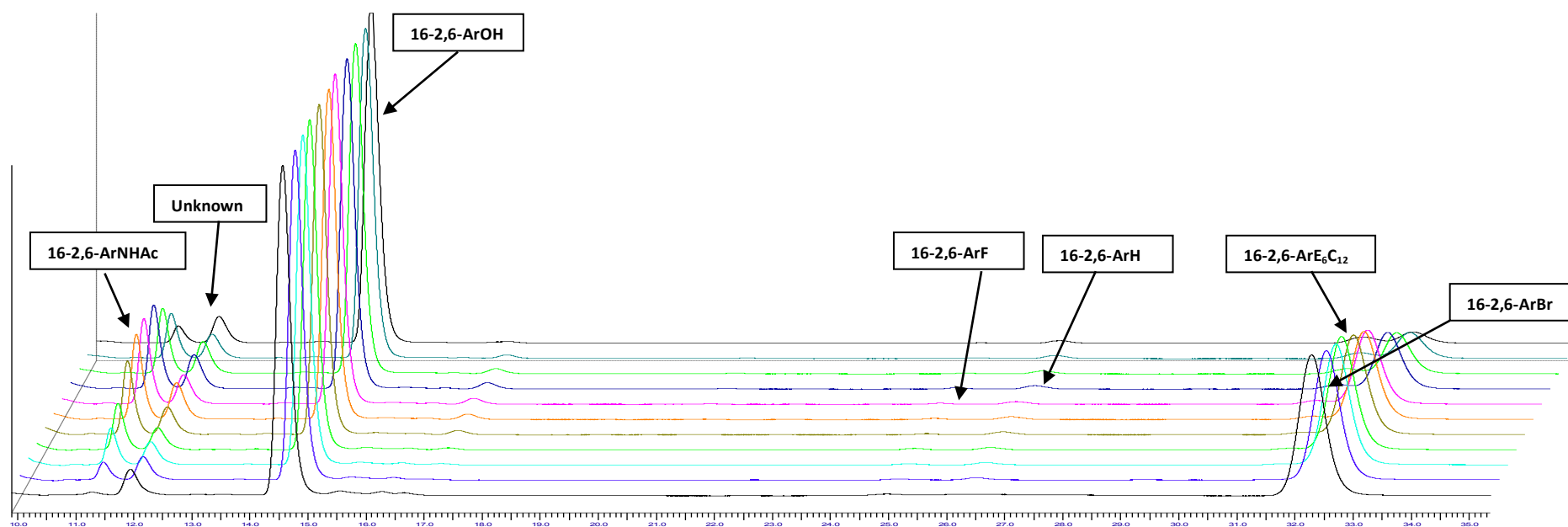


Figure 1S: Chromatograms showing retention times of the various products obtained during dediazotization reaction of 16-2,6-ArN₂⁺ in CTAB/C₁₂E₆ mixed micelles at various mole fractions of C₁₂E₆ (from 0 to 1) at 30 mM total surfactant concentration carried out at 27 ± 0.1 °C and [HBr] = 0.032 M (ca. pH = 1.5). HPLC chromatograms were obtained for product solutions (100 μL) in triplicate at λ = 220 nm using the eluting solvent, 36%/64% (v/v) *i*-PrOH/MeOH with flow rate of 0.40 mL/min.

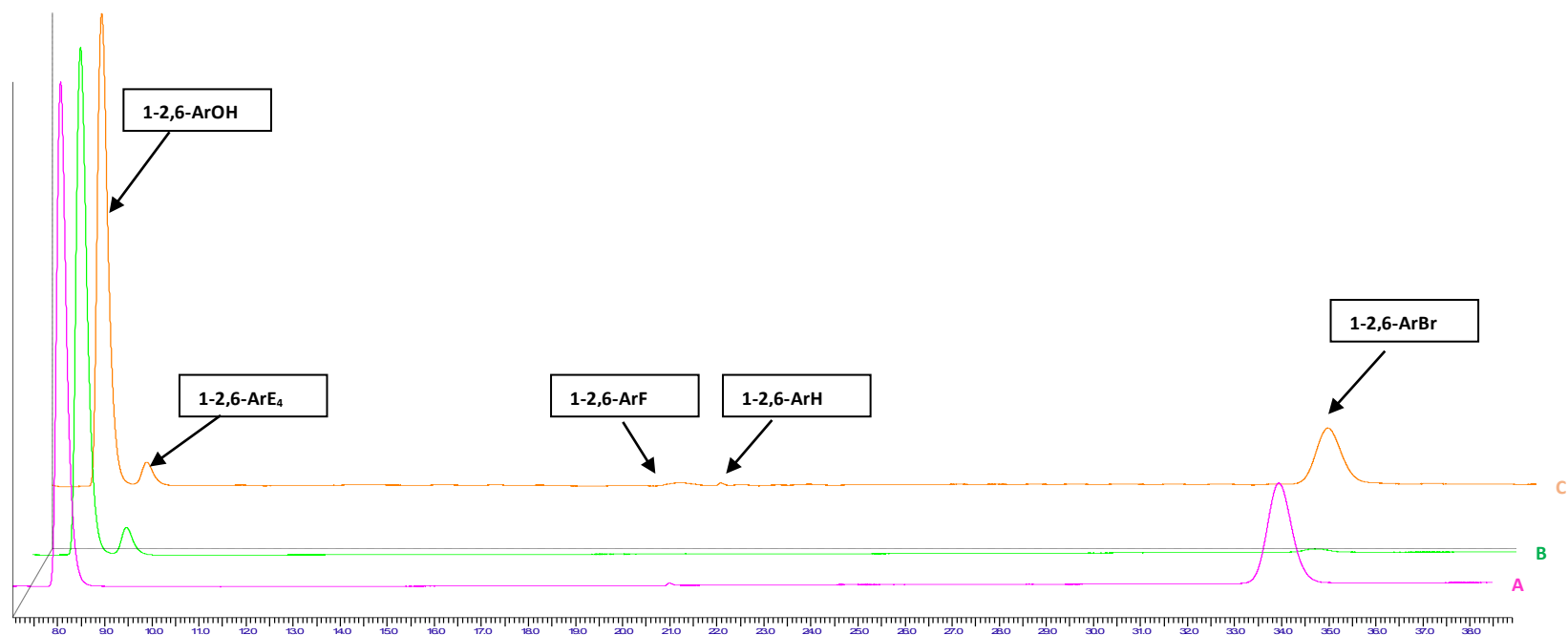


Figure 2S: Chromatograms showing retention times of the various products obtained during dediazonation of 1-2,6- ArN_2^+ in TMABr (A); in E_4 (B); and TMABr/ E_4 mixture at TMABr mole fraction ≈ 0.2 (C) at total [TMABr] or [E_4] or [TMABr + E_4] of 2.5 M at 27 ± 0.1 °C and [HBr] = 0.032 M (ca. pH = 1.5). HPLC chromatograms of the samples (50 μL) were obtained in triplicate at $\lambda = 230$ nm using the eluting solvent, 80%/20% (v/v) MeOH/ H_2O at the flow rate of 0.60 mL/min.

Table 1S: HPLC Average peak areas, observed yields, normalized yields for reaction of 16-ArN₂⁺ in aqueous CTAB/C₁₂E₆ solutions at different mole fractions, $X_{C_{12}E_6}$, of C₁₂E₆ in solutions at three different total surfactant concentration of 20, 30 and 40 mM at 27°C and [HBr] = 0.032 M.^a

$X_{C_{12}E_6}$	Peak areas (10 ⁶ μ V.s) ^b							Observed Yields (%) ^c							Normalized Yields (%) ^e				
	16-ArOH	16-ArBr	16-ArE ₆ C ₁₂	16-Ar-F	16-Ar-H	16-Ar-UNK	16-Ar-AcN	16-ArOH	16-ArBr	16-ArE ₆ C ₁₂	16-Ar-F	16-Ar-H	16-Ar-UNK	16-Ar-NHAc	Total ^d	16-ArOH	16-ArBr	16-ArE ₆ C ₁₂	16-Ar-NHAc
20 mM																			
1	26.87	1.289	0.6156	0.0627	0.2123	2.544	0.374	79.0	2.7	1.6	0.3	0.6	5.3	0.8	90.9	94.0	3.2	1.9	0.9
0.9	25.57	2.657	0.4193	0.0952	0.211	1.871	0.799	75.2	5.6	1.1	0.4	0.6	3.9	1.7	89.1	90.0	6.7	1.3	2.0
0.8	24.54	4.438	0.2904	0.0883	0.1958	1.755	1.204	72.2	9.3	0.8	0.4	0.6	3.7	2.5	90.0	85.1	11.0	0.9	3.0
0.7	23.65	5.889	0.2138	0.1044	0.1951	2.102	1.449	69.6	12.4	0.6	0.4	0.6	4.4	3.0	91.5	81.3	14.5	0.7	3.5
0.6	22.62	7.275	0.1497	0.1054	0.2084	1.601	1.612	66.5	15.3	0.4	0.4	0.6	3.3	3.4	90.6	77.7	17.9	0.5	3.9
0.5	21.72	8.985	0.1646	0.6135	0.1715	1.361	1.565	63.9	18.9	0.4	2.6	0.5	2.8	3.3	93.0	73.8	21.9	0.5	3.8
0.4	21.69	10.38	0.0524	0.1121	0.1711	1.25	1.299	63.8	21.9	0.0	0.5	0.5	2.6	2.7	92.5	72.1	24.7	0.1	3.1
0.3	21.09	12.04	0.0383	0.1005	0.1501	1.233	1.115	62.0	25.4	0.0	0.4	0.4	2.6	2.3	93.7	69.1	28.3	0.0	2.6
0.2	21.09	13.43	0	0.1045	0.1341	1.25	6.788	62.0	28.3	0.0	0.4	0.4	2.6	1.4	95.7	67.6	30.8	0.0	1.5
0.1	20.35	14.44	0	0.1015	0.1445	1.265	3.728	59.9	30.5	0.0	0.4	0.4	2.6	0.8	95.0	65.7	33.4	0.0	0.9
0	20.86	16.33	0	0.1197	0.4141	1.232	0.639	61.4	34.5	0.0	0.5	0.1	2.6	0.1	99.3	63.9	35.9	0.0	0.1
30 mM																			
1	26.50	1.273	0.6065	0.0921	0.0539	2.015	1.018	78.0	2.7	1.5	0.4	0.2	4.2	2.1	89.2	92.5	3.2	1.8	2.5
0.9	23.24	2.921	0.3928	0.0872	0.2061	1.599	2.444	68.4	6.1	1.0	0.4	0.6	3.3	5.1	85.5	84.8	7.6	1.3	6.3
0.8	21.90	4.642	0.2593	0.0881	0.2099	1.989	3.37	64.4	9.8	0.7	0.4	0.6	4.1	7.0	87.7	78.7	11.9	0.8	8.6
0.7	20.03	6.029	0.1828	0.1312	0.217	1.969	4.073	58.9	12.7	0.5	0.6	0.6	4.1	8.5	86.6	73.1	15.8	0.6	10.5
0.6	19.15	7.755	0.0558	0.0914	0.253	1.587	4.004	56.3	16.3	0.2	0.4	0.7	3.3	8.4	86.4	69.4	20.1	0.2	10.3
0.5	18.56	9.105	0.0433	0.0978	0.2525	1.976	3.864	54.6	19.2	0.1	0.4	0.7	4.1	8.1	88.0	66.6	23.4	0.2	9.8
0.4	18.49	10.33	0.0251	0.0942	0.2558	1.448	3.259	54.4	21.8	0.1	0.4	0.8	3.0	6.8	88.0	65.5	26.2	0.1	8.2
0.3	19.40	12.51	0.0248	0.118	0.3101	1.243	2.131	57.1	26.4	0.1	0.5	0.9	2.6	4.4	92.9	64.9	30.0	0.1	5.1
0.2	19.13	13.20	0.0121	0.0868	0.2922	1.296	1.649	56.3	27.8	0.1	0.4	0.9	2.7	3.4	92.4	64.2	31.8	0.1	3.9
0.1	19.94	14.74	0.0094	0.0963	0.3377	1.389	0.818	58.7	31.1	0.1	0.4	1.0	2.9	1.7	96.8	64.1	34.0	0.1	1.9
0	20.04	16.27	0	0.0607	0.3304	1.588	0.142	58.9	34.4	0.0	0.3	1.0	3.3	0.3	99.2	62.9	36.7	0.0	0.3

40 mM																			
1	25.92	1.298	0.5951	0.0542	0.6513	1.606	1.346	76.3	2.7	1.5	0.2	1.9	3.4	2.8	90.7	91.6	3.3	1.8	3.4
0.9	21.44	2.843	0.4331	0.011	0.5486	2.056	4.074	63.1	6.0	1.1	0.5	1.6	4.3	8.5	86.6	80.2	7.6	1.4	10.8
0.8	19.2	4.474	0.3317	0.0457	0.2355	2.124	5.629	56.5	9.4	0.9	0.2	0.7	4.4	11.7	84.5	72.0	12.0	1.1	15.0
0.7	17.33	5.692	0.2119	0.0885	0.5372	1.994	6.271	51.0	12.0	0.6	0.4	1.6	4.2	13.1	84.3	66.5	15.7	0.7	17.1
0.6	14.96	7.604	0.123	0.0855	0.5634	2.409	6.206	44.0	16.0	0.3	0.4	1.7	5.0	12.9	82.0	60.0	21.9	0.5	17.7
0.5	14.81	9.277	0.0529	0.1639	0.9179	2.284	6.096	43.6	19.6	0.2	0.4	2.7	4.8	12.7	86.6	57.3	25.7	0.2	16.7
0.4	15.79	10.40	0.0459	0.1003	0.3605	2.826	4.869	46.5	21.9	0.1	0.4	1.1	5.9	10.2	87.1	59.0	27.9	0.2	12.9
0.3	16.38	11.64	0.0273	0.0999	0.3474	2.593	3.885	48.2	24.6	0.1	0.4	1.0	5.4	8.1	88.8	59.5	30.3	0.1	10.0
0.2	17.96	13.20	0.0113	0.0961	0.2971	2.772	2.121	52.9	27.9	0.1	0.4	0.9	5.8	4.4	93.1	62.0	32.7	0.1	5.2
0.1	18.12	14.86	0.0136	0.0879	0.1785	2.657	1.067	53.3	31.4	0.1	0.4	0.5	5.5	2.2	93.9	61.3	36.1	0.1	2.6
0	18.96	16.67	0	0.0942	0.1365	2.799	0.132	55.8	35.2	0.0	0.4	0.4	5.8	0.3	98.4	61.1	38.6	0.0	0.3

^aReaction time ca. 48 h to ensure complete dediazonation. [16-2,6-ArN₂BF₄] was ca. 3.2 x 10⁻⁴ M in all solutions.

^b100 μL sample injections. Peak areas are average of triplicate injections. Eluting solvents: 65%MeOH/35%*i*-PrOH; Flow rate: 0.4 ml/min; Detector wavelength: λ = 220 nm.

^c% observed yields were calculated as: % [16-2,6-ArX] = 100[16-2,6-ArX]/[16-2,6-ArN₂⁺] where X = -OH, -Br, -F, -H, -NHAc, -E₆C₁₂, UNK (which is unknown); Concentrations (in M) of products were determined by HPLC calibration curves of purified products using equations; [16-2,6-ArOH] = (peak area in μV.s + 28660)/(10¹¹)*; [16-2,6-ArBr] = (peak area in μV.s - 14530)/(1.393 × 10¹¹)*; [16-2,6-ArH] = (Peak area in μV.s - 14590)/(9.883 × 10¹⁰)*; [16-2,6-ArF] = (Peak area in μV.s)/(6.955 × 10¹⁰)*; [16-2,6-ArNHAc] = (Peak area in μV.s)/(1.416 × 10¹⁰)*; [16-2,6-ArE₆C₁₂] = (Peak area in μV.s x 0.8435 x 10⁻¹¹ + 1.13 x 10⁻⁷) and [16-2,6-ArUNK] = (Peak area in μV.s)/(1.416 x 10¹⁰) taken same as acetonitrile product to get a rough estimate. Calibration curve correlation coefficient was > 0.99.

* Zhang, Y. L.; Romsted, L. S.; Zhuang, L. Z.; de Jong, S. *Langmuir* **2013**, *29*, 534.

^d% Total = %16-2,6-ArOH + %16-2,6-ArBr + 2 %16-2,6-ArH + %16-2,6-ArF + %16-2,6-ArNHAc + %16-2,6-ArUNK

^e normalized yields; % 16-2,6-ArX = 100 (%16-2,6-ArX)/(%16-2,6-ArOH + %16-2,6-ArBr + %16-2,6-ArE₆C₁₂ + %16-2,6-ArNHAc); where X = -OH, -Br, -NHAc, -E₆C₁₂

Table 2S: HPLC Average peak areas, observed yields, normalized yields for reaction of 1-ArN₂⁺ in aqueous TMABr/E₄ solutions at different mole fractions, X_{E4} (= 1-X_{TMABr}), of tetraethylene glycol, E₄, in solutions at total TMABr and E₄ concentration of 2.5 M at 27°C and [HBr] = 0.032 M.^a

X _{E4}	[E ₄]	[Br _T] ^b	[H ₂ O]	Peak Areas (10 ⁶ μV.s) ^c					Observed Yields ^d (%)					Normalized Yields (%) ^e			S _w ^{Br f}	[H ₂ O]/[Br _T]	
	M	M	M	1-2,6-ArOH	1-2,6-ArBr	1-2,6-ArE ₄	1-2,6-ArF	1-2,6-ArH	1-2,6-ArOH	1-2,6-ArBr	1-2,6-ArE ₄	1-2,6-ArF	1-2,6-ArH	Total	1-2,6-ArOH	1-2,6-ArBr			1-2,6-ArE ₄
0.98	2.45	0.08	35.27	7.86	0.75	3.38	0.019	0.023	80.05	4.16	9.64	1.23	0.84	96.77	85.43	4.39	10.18	21.93	0.05
0.93	2.32	0.21	34.48	7.64	1.68	3.48	0.019	0.045	77.71	9.49	9.94	1.26	1.60	101.59	80.33	9.61	10.06	19.96	0.12
0.90	2.25	0.28	33.81	6.86	1.98	3.34	0.015	0.088	69.75	11.15	9.56	0.95	3.14	97.69	77.87	11.92	10.21	18.40	0.15
0.80	2.00	0.53	34.25	6.04	2.88	2.63	0.008	0.052	61.41	16.31	7.53	0.46	1.86	89.42	72.63	18.73	8.64	16.81	0.26
0.69	1.75	0.80	34.41	5.41	3.47	1.85	0.023	0.117	55.04	19.69	5.28	1.50	4.17	89.86	70.34	23.38	6.28	14.26	0.33
0.59	1.50	1.07	34.50	4.56	4.18	1.48	0.021	0.139	46.38	23.75	4.24	1.38	4.98	85.71	64.73	29.93	5.34	14.91	0.46
0.49	1.25	1.31	34.95	4.37	3.61	1.11	0.080	0.220	44.42	20.45	3.16	5.19	7.92	89.06	68.91	26.93	4.16	10.40	0.39
0.40	1.00	1.52	35.60	4.19	4.41	0.68	0.031	0.277	42.62	25.04	1.93	2.01	9.93	91.45	66.08	31.49	2.43	11.19	0.48
0.30	0.75	1.78	37.42	3.90	4.31	0.30	0.036	0.422	39.62	24.47	0.86	2.32	15.11	97.50	68.37	30.56	1.07	9.38	0.45
0.20	0.50	2.04	39.18	5.04	5.25	0.13	0.022	0.191	51.26	29.80	0.37	1.41	6.84	96.52	65.82	33.76	0.42	9.84	0.51
0.10	0.25	2.28	39.72	5.47	5.60	0.02	0.037	0.108	55.61	31.81	0.06	2.42	3.89	97.66	65.12	34.82	0.07	9.32	0.53
0.03	0.07	2.46	39.77	5.49	5.85	0.00	0.029	0.044	55.85	33.27	0.00	1.89	1.58	94.17	63.32	36.68	0.00	9.12	0.58

a. Reaction time ca. 48 hours. The concentrations of 1-2,6-ArN₂BF₄ were around 2 x 10⁻³ M but vary in each experiment. 50 μl of cyclohexane was layered on top of TMABr/E₄ solutions in 2 ml volumetric flasks to prevent the evaporation of 1-ArBr. Prior to HPLC analysis, the product mixture was diluted 5 fold with methanol to dissolve both the cyclohexane and the aqueous salt solution.

b. [Br_T] = [TMABr] + 0.032 M HBr

c. 50 μL sample injections. Peak areas are average of triplicate injections. Eluting solvents: 80%MeOH/20%*i*-PrOH; Flow rate: 0.6 ml/min; Detector wavelength: 230 nm.

d. % observed yields were calculated as: % [1-2,6-ArX] = 50 [1-2,6-ArX] / [1-2,6-ArN₂⁺] where X = -OH, -Br, -F, -H, -E₄; Concentrations (in M) of products were determined by HPLC calibration curves of purified products using equations; [1-2,6-ArOH] = (peak area in μV.s) / (1.3 x 10¹⁰)^{*}; [1-2,6-ArBr] = (peak area in μV.s - 14530) / (2.31 x 10¹⁰)^{*}; [1-2,6-ArH] = (Peak area in μV.s) / (2.7 x 10¹⁰)^{*}; [1-2,6-ArF] = (Peak area in μV.s) / (4.9 x 10¹⁰)^{*}; [1-2,6-ArE₄] = (Peak area in μV.s) / (4.62 x 10¹¹). Correlation coefficient calibration curve was > 0.99. All these equations are reported in *Laurence S. Romsted and Jihu Yao*, *Langmuir*, 1996, 12, 2425–2432.

e. Normalized yield were calculated by % 1-2,6-ArX = 100 (%1-2,6-ArX) / (%1-2,6-ArOH + %1-2,6-ArBr + %1-2,6-ArE₄ + %1-2,6-ArH); where X = -OH, -Br, -E₄.

f. S_w^{Br} = ([H₂O](%1-2,6-ArBr)) / ([Br_T](%1-2,6-ArOH))

Figure 3S: Plot between (a) total bromide ion concentration, $[Br_t^-]$ and 1-2,6-ArBr normalized %yield fitted to equation $[Br_t^-] = -0.220 + 0.220e^{-(1-2,6-ArBr \% yield)/14.45}$; and (b) selectivity of 1-2,6-ArN₂⁺ ion towards bromide ions relative to water, S_W^{Br} fitted to the equation: $S_W^{Br} = 7.927 + 13.92e^{-[Br_t^-]/0.944}$ as a function of mole fraction of TMABr in TMABr + E₄ mixture at 27 °C.

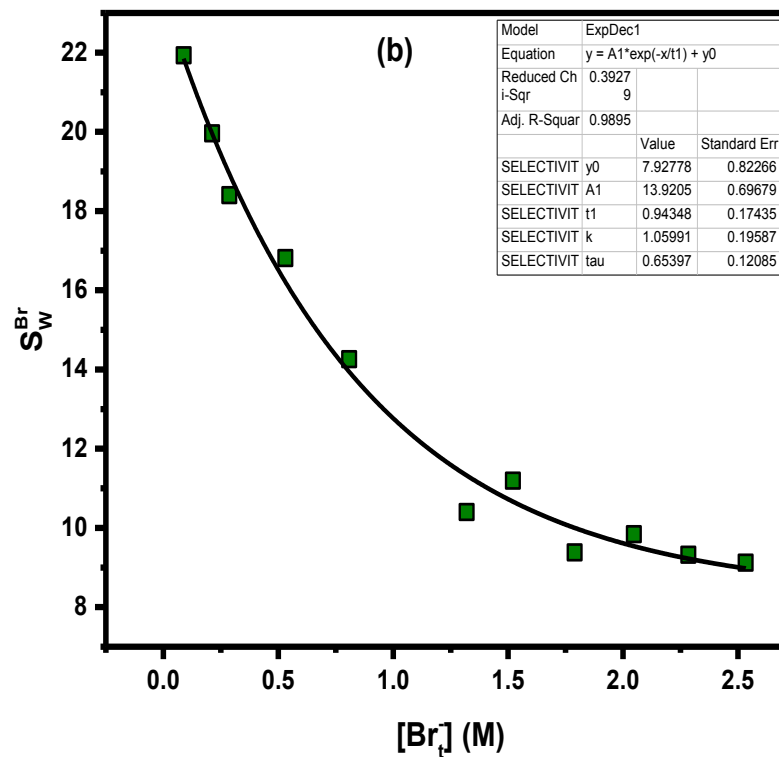
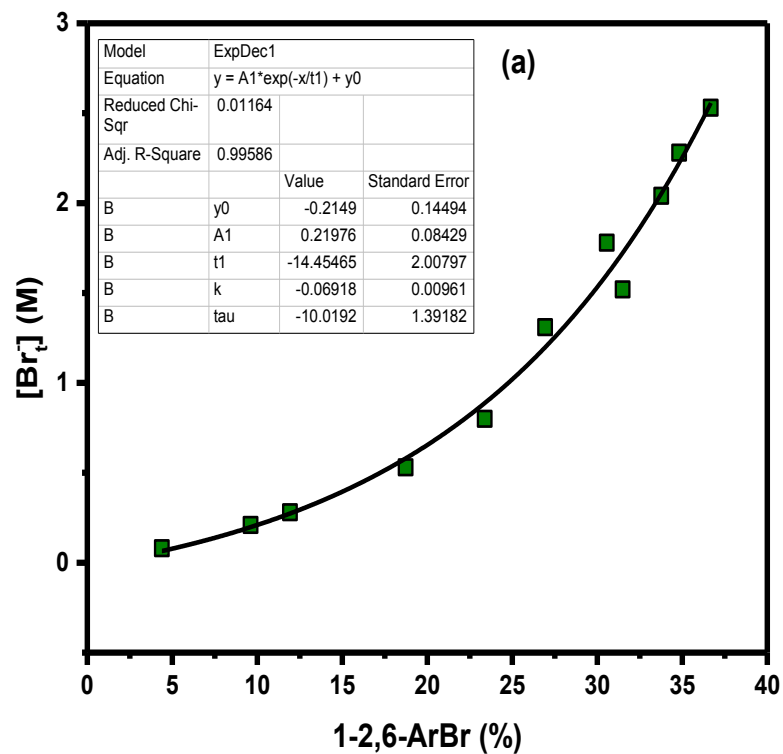


Table 3S: Estimated values of interfacial molarities of bromide ions^a and water^b ((Br)_m and (H₂O)_m) in aqueous CTAB/C₁₂E₆ solutions at different mole fractions, X_{C₁₂E₆}, of C₁₂E₆ in solutions at three different total surfactant concentration of 20, 30 and 40 mM at 27°C and [HBr] = 0.032 M.

X _{C₁₂E₆}	(H ₂ O) _m	(Br) _m	(H ₂ O) _m	(Br) _m	(H ₂ O) _m	(Br) _m
	20 mM		30 mM		40 mM	
	1	30.69	0.06	30.41	0.06	30.30
0.9	36.92	0.13	34.52	0.16	32.64	0.16
0.8	37.96	0.26	34.41	0.29	31.51	0.29
0.7	38.66	0.38	33.94	0.44	30.85	0.43
0.6	39.03	0.54	34.10	0.67	30.08	0.78
0.5	38.90	0.78	33.91	0.89	29.87	1.09
0.4	38.81	1.00	34.29	1.13	31.44	1.30
0.3	38.34	1.34	35.40	1.54	32.63	1.58
0.2	38.15	1.64	35.93	1.77	35.22	1.90
0.1	38.27	2.00	37.26	2.09	37.32	2.45
0	38.85	2.42	38.96	2.57	39.13	2.95

- Equation used to estimate interfacial bromide ion molarity: $(\text{Br})_m = -0.220 + 0.220e^{-(16-2,6-\text{ArBr \% yield})/14.45}$
- Equation used to estimate interfacial water molarity: $(\text{H}_2\text{O})_m = S_w^{\text{Br}} \times (\text{Br})_m (\%16-2,6-\text{ArOH})/(\%16-2,6-\text{ArBr})$

Table 4S: Values of rate constants, A_i 's and the percent contributions of each rate constant to overall rate obtained by fitting kinetic data for reaction of 16 – ArN₂⁺ and TBHQ in mixed micelles to equation (3). The total surfactant concentration was fixed at 20 mM, 30 mM and 40 mM and the mole fraction of C₁₂E₆ varied between 0 to 1 in each set of mixed micelles. Reaction conditions were: [16 – ArN₂⁺] = 5.6 x10⁻⁵ M, [TBHQ] = 6.13 x 10⁻⁴ M, [HBr] = 0.032 M (pH = 1.5) and T = 27 °C.

$X_{C_{12}E_6}$	k_{obs}^1	k_{obs}^2	A_1	A_2	r^2	% k_{obs}^1	% k_{obs}^2	k_{obs}^{Av}
[CTAB+C₁₂E₆] = 20 mM								
1.0	0.0045	0.0006	0.033	0.696	0.9999	4.5	95.5	0.0008
0.9	0.0046	0.0011	0.159	0.582	0.9999	21.4	78.6	0.0019
0.8	0.0075	0.0019	0.245	0.513	0.9999	32.4	67.6	0.0037
0.7	0.0094	0.0025	0.310	0.442	0.9999	41.2	58.8	0.0053
0.6	0.0120	0.0033	0.347	0.395	0.9999	46.8	53.2	0.0074
0.5	0.0145	0.0042	0.351	0.364	0.9999	49.1	50.9	0.0093
0.4	0.0183	0.0054	0.365	0.335	0.9999	52.2	47.8	0.0121
0.3	0.0238	0.0069	0.289	0.364	0.9998	44.3	55.7	0.0144
0.2	0.0294	0.0082	0.282	0.347	0.9998	44.9	55.1	0.0177
0.1	0.0340	0.0098	0.356	0.324	0.9999	52.3	47.7	0.0225
0	0.0419	0.0115	0.286	0.347	0.9999	45.2	54.8	0.0252
[CTAB+C₁₂E₆] = 30 mM								
1.0	0.0033	0.0006	0.026	0.802	0.9999	3.1	96.9	0.0007
0.9	0.0047	0.0012	0.127	0.726	0.9999	14.8	85.2	0.0017
0.8	0.0060	0.0017	0.192	0.657	0.9999	22.6	77.4	0.0027
0.7	0.0078	0.0024	0.275	0.573	0.9999	32.5	67.5	0.0042
0.6	0.0084	0.0028	0.288	0.449	0.9999	39.1	60.9	0.0050
0.5	0.0113	0.0037	0.339	0.480	0.9999	41.4	58.6	0.0069
0.4	0.0133	0.0043	0.364	0.450	0.9999	44.7	55.3	0.0083
0.3	0.0159	0.0051	0.351	0.419	0.9999	45.6	54.4	0.0102
0.2	0.0180	0.0059	0.353	0.383	0.9999	48.0	52.0	0.0117
0.1	0.0211	0.0071	0.322	0.317	0.9999	50.4	49.6	0.0142
0	0.0264	0.0080	0.275	0.378	0.9998	42.1	57.9	0.0158

[CTAB+C ₁₂ E ₆] = 40 mM								
1.0	0.0024	0.0006	0.016	0.912	0.9999	1.7	98.3	0.0006
0.9	0.0031	0.0008	0.066	0.846	0.9999	7.2	92.8	0.0010
0.8	0.0040	0.0011	0.141	0.733	0.9999	16.1	83.9	0.0016
0.7	0.0058	0.0019	0.139	0.668	0.9999	17.2	82.8	0.0026
0.6	0.0072	0.0022	0.223	0.623	0.9999	26.4	73.6	0.0035
0.5	0.0086	0.0029	0.198	0.573	0.9998	25.7	74.3	0.0044
0.4	0.0103	0.0031	0.210	0.653	0.9999	24.3	75.7	0.0049
0.3	0.0115	0.0038	0.208	0.623	0.9999	25.0	75.0	0.0057
0.2	0.0144	0.0046	0.287	0.524	0.9999	35.3	64.7	0.0081
0.1	0.0154	0.0052	0.310	0.490	0.9999	38.7	61.3	0.0092
0	0.0176	0.0056	0.326	0.403	0.9998	44.7	55.3	0.0110

Figure 4S: Representative plots of absorbance (Z-axis) vs time (x-axis) for reaction of 1-ArN₂⁺ with TBHQ at different concentrations of TMABr or E₄ (Y-axis) at pH = 3.45 by using HBr at 27 °C.

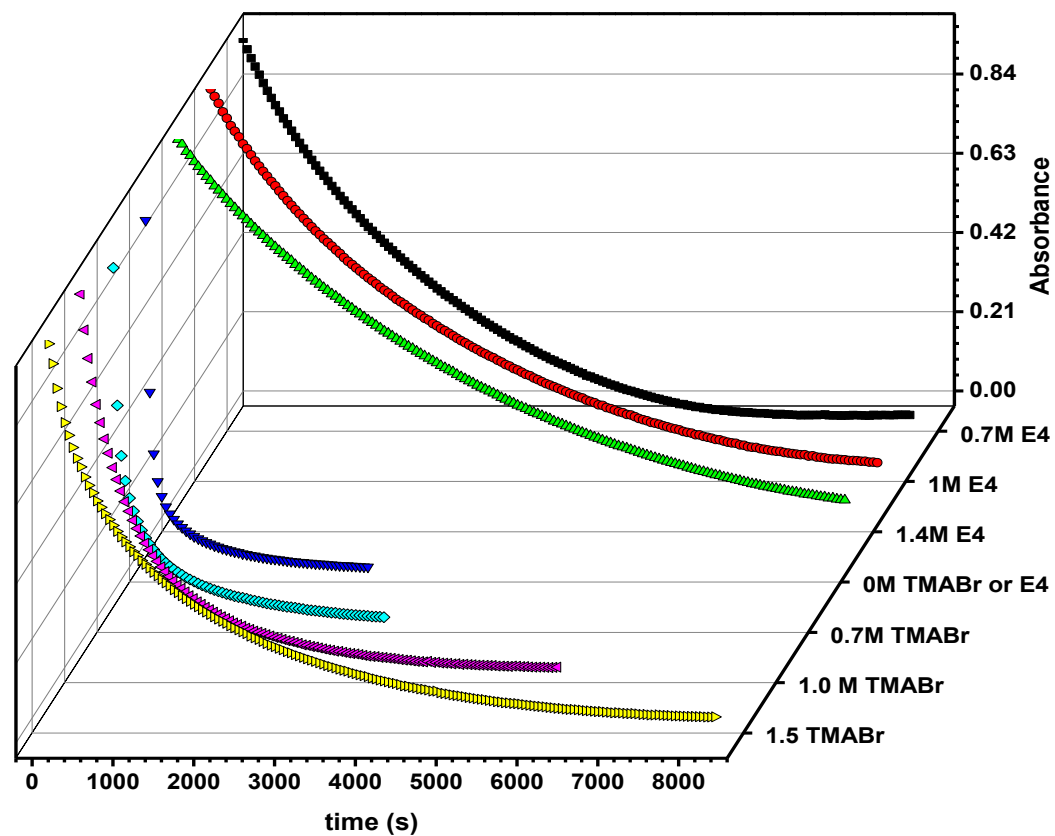


Figure 5S: Representative plots of absorbance vs time of 1-ArN₂⁺ with TBHQ at (a) different mole fractions of TMABr, X_{TMABr} , in mixture of TMABr + E₄ with pH = 3.45 maintained by using HBr and (b) different pH values using different stoichiometric concentrations of HBr while maintaining mole fraction of TMABr in mixture of TMABr + E₄ equal to 0.5 at 27 °C. Total concentration of TMABr + E₄ in all solutions is 1.25 M.

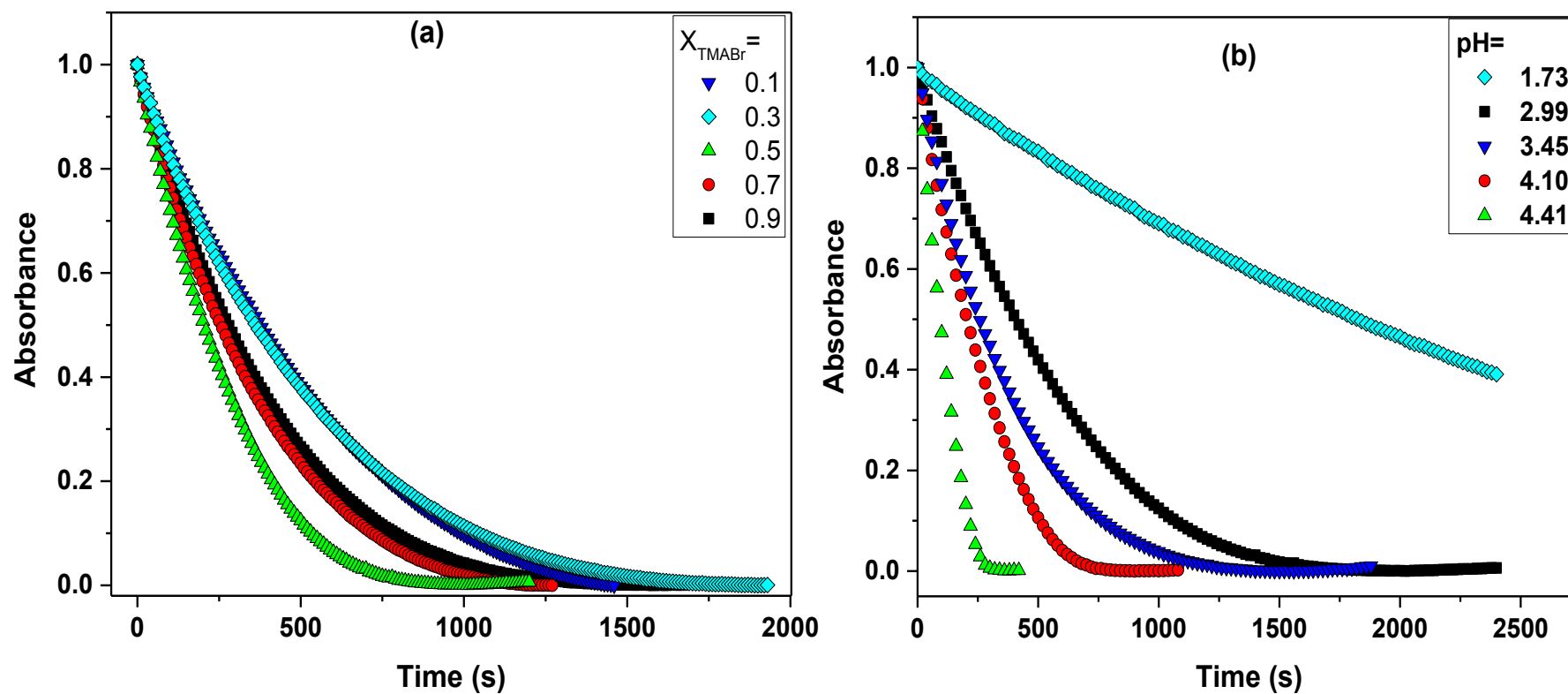


Figure 6S: Variation of the % observed yields of 16-2,6-ArOH and 16-2,6-ArNHAc obtained during chemical trapping experiments as a function of the mole fraction of C₁₂E₆ in CTAB/C₁₂E₆ mixed micelles at three different total surfactant concentrations of 20, 30 and 40 mM at 27 °C.

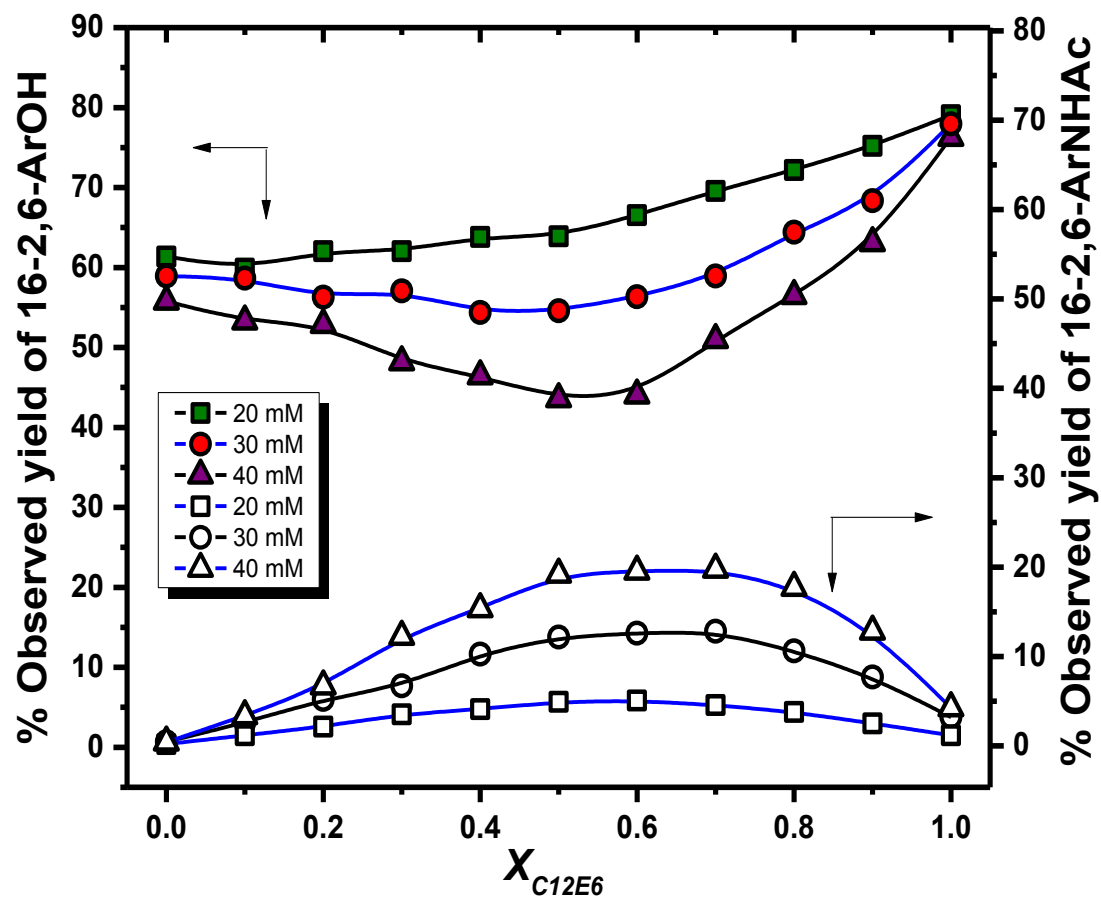


Figure 7S: Variation of k_1' , k_2 and k_3 of reaction between TBHQ^- and 16-ArN_2^+ at micelle-water interface as a function of the mole fraction of C_{12}E_6 in the mixed micelles of CTAB/ C_{12}E_6 at three different total surfactant concentrations of a) 20 mM, b) 30 mM and c) 40 mM at 27 °C.

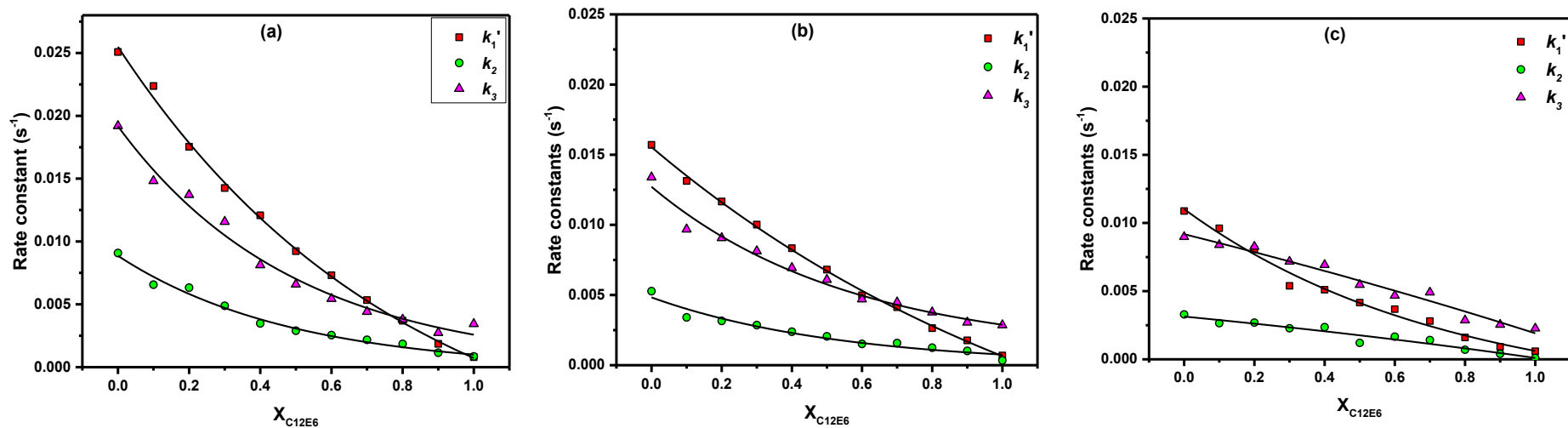
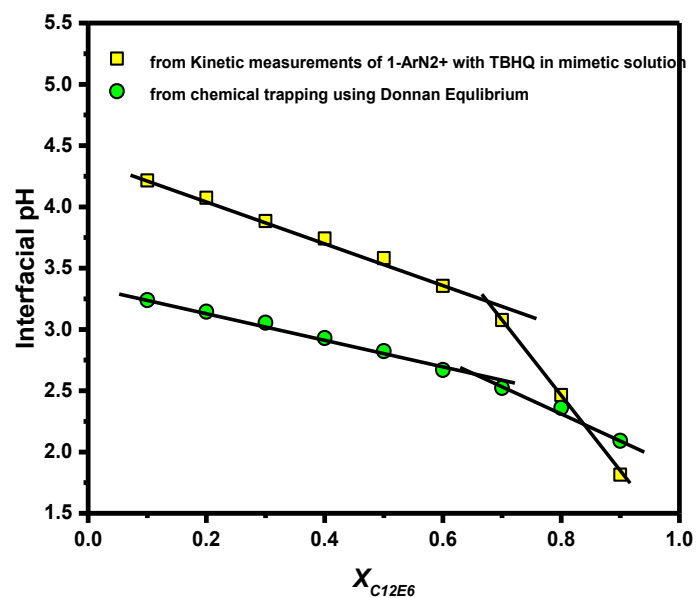


Figure 8S: Estimated interfacial pH in CTAB- $C_{12}E_6$ mixed micelles vs the $X_{C_{12}E_6}$ a) using the $k_{obs(s)}^{Av}$ vs pH variation in the reaction between $1-ArN_2^+$ and TBHQ in the 50/50 TMABr/ E_4 mixture at their total concentration of 1.25 M, and b) from equation 18 obtained from Donnan equilibrium and using the chemical trapping data. The trends in both estimates of $(H)_m$ ($pH = -\log(H)_m$) are the same although the two differ at low $X_{C_{12}E_6}$.



Section 1S. Estimation of the rate constants for the reaction of 16-ArN₂⁺ and TBHQ⁻ in CTAB/C₁₂E₆ mixed micelles shown in Scheme 2.

Benzenediazonium ion, ArN₂⁺, in aqueous solutions is reported to undergo reduction by hydroquinone, HQ, through an overall second-order reaction of ArN₂⁺ and the anion of hydroquinone, Q⁻, in a rate determining step, **Scheme 1**.¹ The rate of the initial fast reaction between Q⁻ and the ArN₂⁺ approaches the diffusion-controlled limit ca. pH 9-10, close to the pK_a of the HQ. The second step is also fast, but its rate depends on the concentration of Q⁻, which is controlled by solution pH. In micellar/microemulsion solutions, the long chain arenediazonium ion, 16-ArN₂⁺, is also reduced by TBHQ through a similar mechanism in the interfacial region.²⁻⁵ The long tail of 16-ArN₂⁺ anchors it within the micellar pseudophase and the charged arenediazonium head group orients it in the interfacial region. The reactions are typically run at pH ≈ 3 to slow the overall reactions sufficiently to run them on a human time scale, seconds to hours. Moreover, > 95% of TBHQ is associated with the interfacial region^{3,6} and correction for partial association of TBHQ to the micelles is not necessary. Under these conditions, the rate equation for the bimolecular reaction within the interfacial region between 16-ArN₂⁺ and TBHQ⁻ in excess of TBHQ is given by:

$$-\frac{d[16\text{-ArN}_2^+]}{dt} = k_1 [16 - \text{ArN}_2^+](\text{TBHQ}^-)_m \Phi_m = k_{obs}[16 - \text{ArN}_2^+] \quad (\text{S1})$$

where k_1 and k_{obs} are the second and pseudo first order rate constants, respectively, where TBHQ is in large excess over 16-ArN₂⁺ insuring first order conditions. Note that square brackets, [], and parentheses, (), indicate molarity in units of moles/liter of solution volume for reaction in bulk solution and in moles per liter of micellar volume for reactions in micelles. In micellar and other association colloid solutions, the volume for the reaction in the micellar pseudophase is proportional to the volume fraction of the surfactant aggregates, Φ_m , and NOT their stoichiometric concentration in solution. Finally, cationic micelles generally increase the interfacial pH (or reduce the interfacial hydrogen ion concentration) thus increasing the degree of

deprotonation of TBHQ and potentially speeding the reaction. Because the reaction is run under pseudo first order conditions, the change in $[16\text{-ArN}_2^+]$ vs time follows a monoexponential equation S2 as per the integrated rate law of the decomposition of reactant:

$$[16 - \text{ArN}_2^+]_t = [16 - \text{ArN}_2^+]_0 e^{-k_{obs}t} \quad (\text{S2})$$

In terms of absorbance values equation S2 converts to

$$A_t = A_\infty + (A_0 - A_\infty)e^{-k_{obs}t} \quad (\text{S3})$$

where A_t , A_∞ and A_0 are the absorbance values at $\lambda = 272$ nm at time t , infinity and zero respectively.

Substantial published evidence⁷⁻¹⁰ indicates that the immediate product of the reaction between polyhydroxylated phenols and ArN_2^+ is a transient diazoether intermediate. Applying this mechanism to the reaction of 16-ArN_2^+ with the antioxidant, TBHQ in the interfacial region of association colloids, **Scheme 2**, begins with rapid and reversible deprotonation followed by the bimolecular reaction between TBHQ^- and 16-ArN_2^+ to form a diazoether intermediate that breaks down into *t*-butylquinone, TBQ, and other products or return to starting materials. The rate equation for the loss of arenediazonium ion between 16-ArN_2^+ , and TBHQ^- within the interfacial region in this mechanism is given by:

$$-\frac{d[16\text{-ArN}_2^+]}{dt} = k_1 [16 - \text{ArN}_2^+](\text{TBHQ}^-)_m \Phi_m - k_2(\text{diazoether})_m \Phi_m \quad (\text{S4})$$

where k_1 and k_2 are the second order rate constants for reaction between TBHQ^- and 16-ArN_2^+ and the first order rate constant of conversion of diazoether adduct back to starting materials respectively in the interfacial region. The $(\text{diazoether})_m$ term is the concentration of intermediate in $\text{mol}\cdot\text{L}^{-1}$ of the interfacial volume. The integrated rate equation¹¹ applicable to the decomposition of 16-ArN_2^+ with time as per the mechanism shown in **scheme 2** under these conditions is given by a biexponential equation S5:

$$[16 - \text{ArN}_2^+]_t = \frac{[16 - \text{ArN}_2^+]_0}{k_{obs}^2 - k_{obs}^1} \left[(k_2 + k_3 - k_{obs}^1) e^{-k_{obs}^1 t} + (k_{obs}^2 - k_2 - k_3) e^{-k_{obs}^2 t} \right] \quad (\text{S5})$$

Where k_{obs}^1 and k_{obs}^2 are two parameters defined in equations S6 and S7 that relate the three experimental rate constants used in the fitting of equation S5.

$$k_{obs}^1 + k_{obs}^2 = k_1' + k_2 + k_3 \quad (\text{S6})$$

$$k_{obs}^1 k_{obs}^2 = k_1' k_3 \quad (\text{S7})$$

Under the pseudo first order conditions i.e., $(\text{TBHQ})_m \gg (16 - \text{ArN}_2^+)$, k_1 is related to k_1' through equation

$$k_1' = k_1 (\text{TBHQ}^-)_m \Phi_m \quad (\text{S8})$$

where k_1 is the second order rate constant between TBHQ^- and $16 - \text{ArN}_2^+$ in the interfacial region, k_1' is the pseudo first order rate constant, and Φ_m is the volume fraction of micellized surfactant.

To convert the equation S5 into measured absorbance, A , values to simulate the kinetic data shown in **Figure 1**, equation S9 that relates the concentration of $16 - \text{ArN}_2^+$ with the measured change in the absorbance at any time t , A_t , at time infinity, A_∞ , and at time = 0, A_0 was used:

$$[16 - \text{ArN}_2^+]_t / [16 - \text{ArN}_2^+]_0 = (A_t - A_\infty) / (A_0 - A_\infty) \quad (\text{S9})$$

Substitution of equation S9 into equation S5 and rearranging (a lot) gives equation S10:

$$A_t = A_\infty + \frac{(A_0 - A_\infty)(k_2 + k_3 - k_{obs}^1)}{k_{obs}^2 - k_{obs}^1} e^{-k_{obs}^1 t} + \frac{(A_0 - A_\infty)(k_{obs}^2 - k_2 - k_3)}{k_{obs}^2 - k_{obs}^1} e^{-k_{obs}^2 t} \quad (\text{S10})$$

Equation S11 is obtained by defining the complex coefficients as parameters, A_1 and A_2 ,

$$A_t = A_\infty + A_1 e^{-k_{obs}^1 t} + A_2 e^{-k_{obs}^2 t} \quad (S11)$$

$$\text{Where } A_1 = \frac{(A_0 - A_\infty)(k_2 + k_3 - k_{obs}^1)}{k_{obs}^2 - k_{obs}^1} \quad (S12)$$

$$\text{and } A_2 = \frac{(A_0 - A_\infty)(k_{obs}^2 - k_2 - k_3)}{k_{obs}^2 - k_{obs}^1} \quad (S13)$$

Equation S11 to S13 are used to fit the absorbance versus time data at each $X_{C_{12}E_6}$ in **Figure 1a**. The values of A_1 , A_2 , k_{obs}^1 and k_{obs}^2 are obtained from the kinetic data in **Figure 1** and listed in **Table 4S** and used to obtain values of k_1' , k_2 and k_3 at each mole fraction of $C_{12}E_6$, in the mixed micellar systems at three different total surfactant concentrations and 27 °C (plotted in **Figure 7S**). Note that under the conditions of $k_3 \gg k_2$, the equation S10 reduces to equation S3 indicating that the reversible formation of diazoether intermediate is the key point for the appearance of biphasic kinetics in the reaction between TBHQ and 16-ArN₂⁺ in the interfacial region because $-d[16\text{-ArN}_2^+]/dt$ depends on the concentration and rate constant for the breakdown of the diazoether intermediate.

Section 2S. Estimation of interfacial hydrogen ion concentration, $(H)_m$, from measured rate constants and the interfacial K_a^m of TBHQ with increasing $X_{C_{12}E_6}$ in mixed CTAB/ $C_{12}E_6$ micelles.

The values of k_1' are related to the $(H)_m$ and the interfacial pH ($pH_m = -\log (H)_m$). The dissociation constant of the TBHQ in the interfacial region, K_a^m , is:

$$K_a^m = \frac{(\text{TBHQ}^-)_m (\text{H})_m}{(\text{TBHQ})_m} \quad (\text{S14})$$

The interfacial acidity constant of TBHQ is defined by the concentration ratio of the acid and base forms of TBHQ within the micellar interface and the hydrogen ion concentration in the interfacial region. We note that this is different from more traditional definitions of the apparent acidity constant, K_{app} , in which the acid and base forms of the indicator are in the interfacial region, but the hydrogen ion concentration is that in the aqueous region, $[\text{H}]_w$. The total mass balance of TBHQ within the interfacial region is given by

$$(\text{TBHQ})_m^T = (\text{TBHQ}^-)_m + (\text{TBHQ})_m \quad (\text{S15})$$

Combining equations S8, S14 and S15 and rearranging yields equation S16:

$$\frac{(\text{TBHQ})_m^T \Phi_m}{k_1'} = \frac{1}{k_1} + \frac{(\text{H})_m}{K_a^m k_1} \quad (\text{S16})$$

Equation S16 is the same as equation 9 in the text.

Knowing that $(\text{TBHQ})_m^T \Phi_m = [\text{TBHQ}]$ in the bulk solution (which was 6.1×10^{-4} M), equation S16 predicts that a plot of $[\text{TBHQ}]/k_1'$ vs the interfacial proton concentration, $(\text{H})_m$ in $\text{mol}\cdot\text{L}^{-1}$ of interfacial volume is linear with intercept equal to $1/k_1$ and slope equal to $1/K_a^m k_1$, see Section 3.3 in text.

Section 3S: Calculation of bulk aqueous bromide ion concentration, $[\text{Br}^-]_w$ from the degree of counterion binding with increasing $X_{\text{C}_{12}\text{E}_6}$ in mixed CTAB/ C_{12}E_6 micelles.

For a given total surfactant concentration the aqueous bromide ion concentration in the CTAB- C_{12}E_6 mixed micellar solution as function of increasing mole fraction of C_{12}E_6 , the aqueous bromide ion concentration is defined as: ¹²

$$[\text{Br}^-]_{\text{W}} = \text{cmc}_{\text{mix}}(1 - X_{\text{C}_{12}\text{E}_6}) + (C_{\text{t}} - \text{cmc}_{\text{mix}})(1 - X_{\text{C}_{12}\text{E}_6})(1 - \beta) + [\text{HBr}] \quad (\text{S17})$$

where cmc_{mix} is the cmc of mixture of surfactants at bulk mole fraction of $X_{\text{C}_{12}\text{E}_6}$ and C_{t} the total surfactant concentration. β is the degree of counterion binding at bulk mole fraction of $X_{\text{C}_{12}\text{E}_6}$ in the solution which was obtained from the data of Hall and Price.¹² $[\text{HBr}]$ is the added HBr concentration (0.032 M) in the solution to get the constant pH (= 1.5) of the solutions. The cmc of aqueous solutions of C_{12}E_6 and CTAB are 0.07 mM and 0.745 mM at 25 °C, respectively.^{13, 14} The cmc values for the mixtures of CTAB with the similar polyoxyethylene based surfactants¹⁵ have been observed to be much less than the cmc of cationic surfactant but very close to the cmc of nonionic surfactant. Therefore cmc_{mix} in all the surfactant solutions, being much below cmc value of CTAB, can be ignored compared to 20 mM, 30 mM and 40 mM total surfactant concentration of the mixtures in equation S17 and equation S17 reduces to equation S18:

$$[\text{Br}^-]_{\text{W}} = C_{\text{t}}(1 - X_{\text{C}_{12}\text{E}_6})(1 - \beta) + [\text{HBr}] \quad (\text{S18})$$

References:

1. K. C. Brown and M. P. Doyle, *J. Org. Chem.*, 1988, **53**, 3255-3261.
2. X. Gao, C. Bravo-Díaz and L. S. Romsted, *Langmuir*, 2013, **29**, 4928-4933.
3. Q. Gu, C. Bravo-Díaz and L. S. Romsted, *J. Colloid Interface Sci.*, 2013, **400**, 41-48.
4. K. Gunaseelan, L. S. Romsted, M. J. P. Gallego, E. Gonzalez-Romero and C. Bravo-Díaz, *Adv. Colloid Interface Sci.*, 2006, **123**, 303-311.
5. K. Gunaseelan, L. S. Romsted, E. González-Romero and C. Bravo-Díaz, *Langmuir*, 2004, **20**, 3047-3055.
6. L. S. Romsted and J. Zhang, *J. Agric. Food. Chem.*, 2002, **50**, 3328-3336.
7. T. J. Broxton and D. L. Roper, *J. Org. Chem.*, 1976, **41**, 2157-2162.
8. M. P. Doyle, C. L. Nesloney, M. S. Shanklin, C. A. Marsh and K. C. Brown, *J. Org. Chem.*, 1989, **54**, 3785-3789.
9. C. Bravo-Díaz, *Diazo hydroxides, diazoethers and related species*, in *Patai's Chemistry of Functional Groups: The Chemistry of Hydroxylamines, Oximes and Hydroxamic Acids*, J. Wiley & Sons, Chichester, UK, 2011.
10. A. Dudzik, K. Jaszczuk, S. Losada-Barreiro and C. Bravo-Díaz, *New J. Chem.*, 2017, **41**, 2534-2542.
11. V. Korobov and V. Ochkov, *Chemical Kinetics with Mathcad and Maple*, SpringerWien, NewYork, 2011.

12. D. G. Hall and T. J. Price, *J. Chem. Soc., Faraday Trans. 1*, 1984, **80**, 1193-1199.
13. E. Fegyver and R. Meszaros, *Soft Matter*, 2014, **10**, 1953-1962.
14. A. A. Dar, G. M. Rather and A. R. Das, *J. Phys. Chem. B*, 2007, **111**, 3122-3132.
15. J. Penfold, E. Staples, P. Cummins, I. Tucker, L. Thompson, R. K. Thomas, E. A. Simister and J. R. Lu, *J. Chem. Soc., Faraday Trans.*, 1996, **92**, 1773-1779.